

# Reasoning with Pixel-level Precision: QVLM Architecture and SQuID Dataset for Quantitative Geospatial Analytics

Peter A. Massih<sup>1,2</sup> & Eric Cosatto<sup>1</sup>

<sup>1</sup>Department of Machine Learning, NEC Laboratories America

<sup>2</sup>EPFL

{pmassih,cosatto}@nec-labs.com, peter.abdelmassih@epfl.ch

## Abstract

*Current Vision-Language Models (VLMs) fail at quantitative spatial reasoning because their architectures destroy pixel-level information required for counting and measurements. Vision encoders compress images through patch embeddings, reducing spatial indexing and losing the precise pixel-level tracking required for accurate counting. We present two contributions to address this fundamental limitation. First, we introduce SQuID (Satellite Quantitative Intelligence Dataset), a benchmark of 2,000 satellite image Question-Answer pairs with both numerical range and categorical answers, designed to evaluate quantitative spatial reasoning. The dataset spans three difficulty tiers with annotations automatically generated from human labels and their learned variability. Second, we propose QVLM (Quantitative Vision-Language Model), a code-generation architecture that maintains pixel precision by decoupling language understanding from visual analysis. Instead of encoding images into embeddings, QVLM generates executable code that first calls a segmentation model to obtain pixel-level masks, then operates directly on these masks, preserving spatial indexing throughout the reasoning process. Our experiments show that QVLM using GPT-5 as coder achieves 42.0% accuracy on SQuID compared to 28.1% for a VLM prompted with image-question pairs. Our work reveals that, for quantitative spatial reasoning, architectural decoupling enables better accuracy on quantitative tasks.*

## 1. Introduction

When a human expert counts buildings in satellite imagery or measures deforested areas, they maintain precise pixel-level tracking throughout their analysis. Each building is indexed, each boundary is traced, and spatial relationships are computed with geometric precision. In contrast, modern Vision-Language Models (VLMs) process these same

images by compressing them through encoders [20, 26] that fundamentally eliminate this pixel-level indexing. The result is a paradox: models that can eloquently describe a forest cannot reliably count its trees.

This limitation has real-world consequences. Climate scientists monitoring deforestation need hectare-precise measurements, not qualitative descriptions. Urban planners assessing solar adoption need accurate counts, not rough estimates. Disaster response teams need building-by-building damage analysis, not vague assessments. Recent comprehensive benchmarks expose this quantitative failure: VLMs achieve only 37-42% accuracy on counting tasks in satellite imagery despite strong performance on qualitative scene understanding [6, 35].

The root cause lies in fundamental architectural constraints. When a 1024×1024 satellite image is processed through a vision encoder, patches (typically 16×16 pixels each) are compressed into a 64×64 grid of tokens—reducing 1,048,576 pixels to 4,096 tokens, a 256-fold compression. This destroys the pixel-level indexing required for quantitative analysis. Recent work quantifies this loss: vision encoders cause 40-60% k-nearest neighbor divergence, meaning nearly half of the local geometric structure disappears during encoding [18]. No amount of training can recover architecturally discarded information.

We present two contributions that address this fundamental limitation:

**SQuID:** A rigorously validated benchmark of multi-resolutions satellite imagery from several public datasets. Unlike existing benchmarks that focus on scene-level understanding [31] or object attributes [16], SQuID specifically tests quantitative spatial reasoning through three difficulty tiers: (i) Basic counting and coverage, (ii) Spatial relationships and proximity, and (iii) Complex multi-condition queries. Each question/answer also includes an acceptable range derived from the variability observed from 10 human annotators.

**QVLM:** An architecture that preserves pixel-level precision by generating executable Python code that orchestrates

segmentation models. Instead of encoding images into embeddings, an LLM generates code that, via APIs, taps into specialized vision modules that produce and analyze pixel-accurate segmentation masks. For example, when asked "How many buildings are within 200m of water?", QVLM generates code that: (1) segments building and water regions, (2) computes spatial relations among them, and (3) counts buildings meeting proximity criteria. This approach, inspired by recent code-generation VLMs [28, 29], maintains complete spatial indexing throughout reasoning.

The implications extend beyond satellite imagery to any domain requiring precise quantitative analysis, from medical imaging requiring millimeter-precise tumor volumes, to robotics requiring exact distance measurements, to precision agriculture requiring plant-level crop quantification. Our work demonstrates that architectural decoupling through code generation and segmentation enables better quantitative spatial reasoning.

**Reproducibility.** To facilitate future research, we publicly release the complete SQuID benchmark with 2,000 questions, ground truth answers, and acceptable ranges at <https://huggingface.co/datasets/PeterAM4/SQuID>, along with the QVLM architecture, evaluation scripts, and DINOv3 segmentation training code at <https://github.com/PeterAMassih/qvlm-squid>.

## 2. Related Work

### 2.1. Quantitative Limitations of VLMs

Recent benchmarks reveal quantitative difficulties across VLM architectures. Danish et al. [6] test models on 31 geospatial tasks, finding that even the best performer (LLaVA-OneVision) achieves only 33.5% accuracy on building counting compared to scene classification having 82.7% accuracy. Zi et al. [35] identify counting as the hardest category across 162,373 question-answer pairs, with leading models achieving only 37.8% accuracy. Zhang and Wang [33] provide detailed failure analysis: mean absolute percentage errors exceeding 87% on tree counting from the NEON dataset, only 7.6% precision for object localization at IoU threshold 0.5 and R<sup>2</sup> values reaching at most 0.35 on counting tasks.

Even specialized remote sensing models display these limitations. Pang et al. [25] report mean absolute errors of 6.75 for counting despite 95% accuracy on image attribute recognition tasks, while Liu et al. [19] report that RemoteCLIP achieved strong scene level and cross modal performance but performs notably worse on dense prediction tasks such as segmentation and detection compared to MIM (Masked Image Modeling) based models.

Moreover, Yuksekgonul et al. [32] expose that VLMs exhibit "bag-of-words behavior," performing at chance on

compositional tasks like distinguishing "grass eating horse" from "horse eating grass." This demonstrates that contrastive pre-training doesn't incentivize compositional understanding and its limited performance on such tasks stems from architectural limitation rather than data insufficiency.

### 2.2. Code Generation for Visual Reasoning

Code generation offers an alternative paradigm that preserves information destroyed by neural encoding. Surís et al. [29] generate Python programs that orchestrate vision APIs, achieving state-of-the-art zero-shot results on compositional reasoning. Subramanian et al. [28] demonstrate the quantitative advantage: nearly 30% higher accuracy on spatial reasoning questions versus baseline VLMs, exactly where end-to-end models fail. Gupta and Kembhavi [8] employ 20+ modules through generated programs for zero-shot compositional reasoning.

These successes suggest explicit program execution maintains spatial precision that neural compression destroys. However, none address satellite imagery's unique challenges: massive resolution disparities from 0.3m to 10m ground-sampling distance (GSD), specialized land-cover categories, and metric-accurate measurements in real-world coordinates.

### 2.3. Segmentation for Quantitative Precision

Recent work demonstrates that segmentation improves quantitative reasoning. Lai et al. [14] discuss "embedding-as-mask," achieving over 20% gIoU improvement by generating segmentation masks during the reasoning process, showing that models cannot answer spatial queries accurately without pixel-level masks. For remote sensing, Kuckreja et al. [13] add grounding tokens producing both textual answers and visual masks, allowing dialogue focused on a specific region.

Zhang et al. [34] show dramatic improvements through architecture alone: orchestrating Grounding DINO, SAM, and CLIP achieves 31-225% improvement over vanilla SAM across remote sensing datasets without domain-specific training. Li et al. [17] improve segmentation quality by 5-15% in four major tasks (semantic segmentation, building extraction, road extraction, and flood detection) by upsampling features that functions similarly to segmentation, restoring spatial information and recovering fine pixel-level details typically lost in standard encoders.

Our QVLM architecture leverages these advances by operating directly on segmentation masks through executable code.

### 2.4. Positioning SQuID

Existing benchmarks only partly test quantitative spatial reasoning. EarthVQA focuses on relational Visual Question Answering (VQA) for remote-sensing scenes, with 208,593

question answer pairs across 6,000 images [31]. HRVQA includes 1,070,240 pairs on 53,512 high-resolution aerial images, focusing mainly on object presence and attributes rather than relationships or measurements [16]. SpatialVLM [2] adds spatial reasoning to Vision-Language Models trained mostly on everyday natural-image datasets, not on aerial satellite imagery.

Beyond remote sensing, modern VLMs still struggle with compositional reasoning (CR), the ability to combine multiple pieces of information, such as objects, their attributes, and how they relate to each other. They often fail on multi-step tasks, where solving a question requires several reasoning steps (for example, “count buildings within 200 m of water areas”) [9, 32]. SQuID fills this gap. It is designed to test quantitative spatial reasoning across three difficulty tiers, with each numeric question including human validated answer ranges derived from 10 annotators.

### 3. The SQuID Dataset

To evaluate quantitative spatial reasoning in satellite imagery, we introduce SQuID (Satellite Quantitative Intelligence Dataset), a benchmark of 2,000 questions across 587 satellite images spanning three difficulty tiers. Unlike existing remote sensing VQA datasets that emphasize scene-level understanding [31] or object attributes [16], SQuID specifically targets quantitative spatial reasoning: counting, measuring, and computing spatial relationships with metric precision.

#### 3.1. Dataset Construction

SQuID combines automatic generation from segmentation masks with human annotation to achieve both scale and validation. We algorithmically generate questions from three established remote sensing datasets with segmentation masks: DeepGlobe [7] (174 images, 0.5m GSD, 6-class land cover), EarthVQA [31] (364 images, 0.3m GSD, 5-class segmentation), and Solar Panels [10] (35 images, 0.3m GSD, photovoltaic masks). To avoid contamination, we only use images from published validation partitions. Our generation pipeline: (1) extracts connected components using OpenCV contour detection, (2) computes geometric properties in metric units based on GSD, (3) performs spatial operations (distance transforms, buffering, intersection), and (4) generates questions with ground-truth answers derived from mask geometry. We explicitly include minimum area thresholds in counting questions and intentionally include questions with zero-valued answers to test robustness to feature absence.

To validate our automatic generation, we collected human annotations on 50 USGS NAIP [22] images at 1.0m GSD. Using a custom grid-based annotation interface built on Turkle [11], 10 independent annotators marked spatial regions, provided counts or selected categorical answers

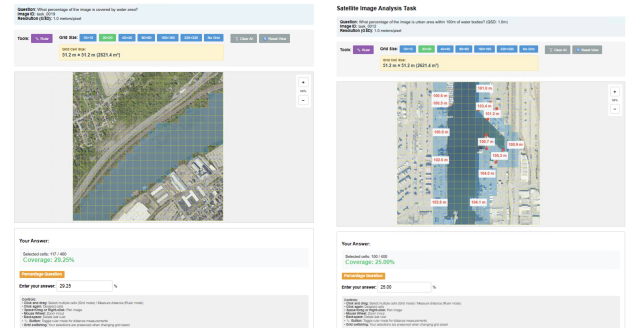


**Figure 1. Grid-based annotation interface built on Turkle with adjustable resolution (10x10 to 320x320).** (a) Annotators select grid cells covering target land-cover classes to answer percentage questions. (b) Distance ruler tool enables precise measurements for proximity-based questions.

\*Questions abbreviated for space, see supplementary material for complete examples.

**Table 1.** Inter-rater reliability by question type (500 annotations from 50 questions  $\times$  10 annotators).

Type	N	Krippendorff's $\alpha$	ICC(2,k)
Percentage	26	0.832	0.930
Count	12	0.959	1.059*
Proximity	9	0.424	0.517
Numeric	47	0.79	0.84
Categorical <sup>†</sup>	3	—	—

\*ICC(2,k) > 1.0 can occur with high consistency. <sup>†</sup>Use majority voting.

(Figure 1). From 500 total annotations, we compute inter-rater reliability using Krippendorff's  $\alpha$ , obtaining 0.79 overall [12]. Table 1 shows reliability by question type, with count questions obtaining highest agreement ( $\alpha = 0.959$ ) and proximity questions lowest ( $\alpha = 0.424$ ).

#### 3.2. Question Types and Difficulty Tiers

SQuID organizes questions into three difficulty tiers that progressively test spatial reasoning capabilities (see Figure 3):

**Tier 1: Basic Quantification.** Single-step analysis on individual land cover classes: coverage percentages, region counting, size measurements, and presence/absence verification. These questions test fundamental spatial perception without requiring cross-class relationships.

**Tier 2: Spatial Relationships.** Multi-class spatial analysis requiring distance computations, proximity assessments, connectivity detection, and fragmentation analysis. Questions involve explicit metric distances and spatial relationships between different land cover types.

**Tier 3: Complex Multi-Condition.** Compositional reasoning requiring multiple filtering and intersection operations. These questions combine size thresholds, proxim-

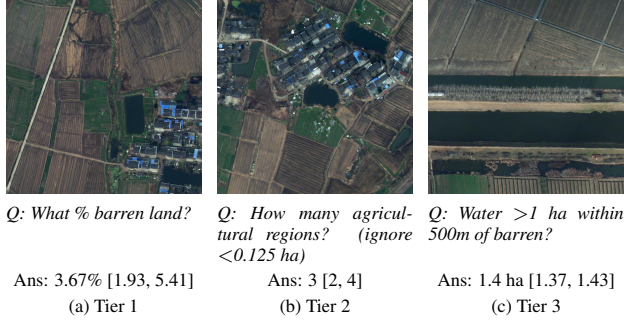


Figure 2. **SQuID examples across difficulty tiers.** (a) Basic quantification: single-step percentage calculation. (b) Spatial relationships: counting with size filtering. (c) Complex multi-condition: size filtering + distance transform + intersection (GSD: 0.3m for all).

*Note: Questions shown here are abbreviated for layout.*

ity constraints, and area calculations where multiple spatial conditions must be simultaneously satisfied.

Table 2 shows representative questions from each tier with their acceptable answer ranges, demonstrating the progression from basic single-step queries to complex multi-conditional reasoning. Figure 2 shows visual examples from actual benchmark images.

### 3.3. Human-Validated Acceptable Ranges

A key innovation in SQuID is the use of acceptable answer ranges rather than point estimates. Given an image at a fixed resolution, human spatial perception naturally varies and different annotators may count slightly different numbers or segment slightly different boundaries. To capture this variability, we compute Median Absolute Deviation (MAD) [15] on our 500 human-generated annotations:

$$\text{MAD} = \text{median}(|X_i - \text{median}(X)|) \quad (1)$$

where  $X = \{X_1, X_2, \dots, X_n\}$  represents the set of  $n$  answers for a given question, and  $X_i$  is an individual annotator's response. MAD achieves a 50% breakdown point, the highest possible for any scale estimator—remaining stable even when up to 50% of annotations are outliers.

From 26 basic ‘Percentage’ questions (260 annotations), we obtain a mean  $\text{MAD} = 1.735$  that define acceptable ranges given by:  $\text{range}(P) = [P - \text{MAD}, P + \text{MAD}]$ . We further distinguish 9 ‘Proximity’ questions (90 annotations) that include complex distance estimation, for those we get a larger  $\text{MAD} = 2.250$ .

For ‘Count’ questions, we normalize the range to the magnitude of the median of the counts:

$$\text{MADc} = \frac{\text{median}(|X_i - \text{median}(X)|)}{\text{median}(X)} \quad (2)$$

From the 120 ‘Count’ annotations, we obtain a mean

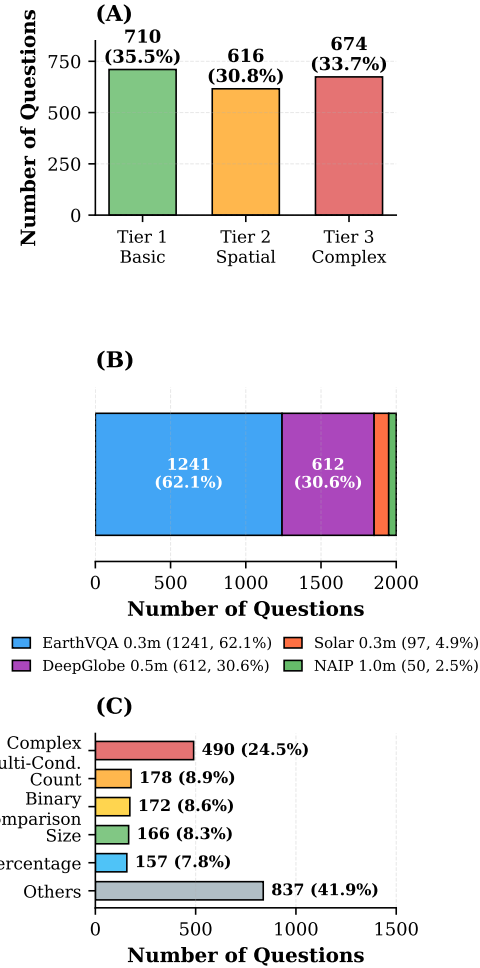


Figure 3. **SQuID dataset composition.** (A) Three difficulty tiers. (B) Four data sources at 0.3m–1.0m GSD. (C) Top 5 question categories and percentage contribution of all others question types

$\text{MADc} = 0.19$ . The ranges for a ‘Count’ question with answer  $C$  are given by:  $\text{range}(C) = [C - C \times \text{MADc}, C + C \times \text{MADc}]$ . This way, a larger count induces a larger range, reflecting its greater natural variability. As for the remaining non-numeric questions, no ranges are calculated as an exact match is required.

### 3.4. Quality Assurance

To ensure evaluation integrity in SQuID, we follow several guidelines: (1) **Explicit area thresholds:** questions must state minimum area thresholds, preventing ambiguity between segmentation artifacts and actual objects. (2) **Metric consistency:** questions with distance computations must explicitly state GSD to ensure correct metric calculations. (3) **Zero-value inclusion:** unlike benchmarks with only positive examples, some questions have zero-valued ground truth, testing whether models correctly identify feature absence (102 zero valued questions).

Table 2. Representative questions from SQuID across three difficulty tiers. Acceptable ranges derived from human annotation variance (MAD:  $\pm 1.735\%$  for percentages,  $\pm 0.50$  for counts,  $\pm 2.250\%$  for proximity).

Tier	Type	Question	Answer	Range	GSD
<b>Tier 1: Basic Quantification</b>					
1	percentage	What percentage of the image is covered by barren land?	33.13%	[31.4, 34.87]	0.3m
1	count	How many buildings are there? (ignore $<0.01$ ha)	4	[3, 5]	0.3m
1	binary	Is there more water than barren land?	yes	exact	0.3m
<b>Tier 2: Spatial Relationships</b>					
2	proximity	What % agricultural land within 50m of grassland?	4.84%	[2.59, 7.09]	0.5m
2	flood risk	Buildings within 100m of water (flood risk)?	14	[11, 17]	0.3m
<b>Tier 3: Complex Multi-Condition</b>					
3	multi-cond.	Find water $>5$ ha, calc area within 200m of grassland	7.78 ha	[7.6, 7.96]	0.3m
3	urban risk	Find urban $>1$ ha, calc area within 100m of water	17.75 ha	[17.35, 18.15]	0.5m

Questions abbreviated for space; complete examples and all questions type in supplementary material.

**(4) Range validation:** we verify ground truth answers fall within physically plausible bounds and acceptable ranges don't extend beyond these bounds.

## 4. QVLM

### 4.1. Model Architecture

QVLM addresses the quantitative reasoning failure of traditional Vision-Language Models through architectural decoupling. Instead of compressing images through vision encoders that destroy pixel-level spatial indexing, QVLM generates executable code that orchestrates specialized segmentation models operating directly on pixel accurate masks.

The architecture follows three stages: (1) an LLM interprets the natural language question and generates Python code invoking spatial analysis functions, (2) the code calls a segmentation model to extract pixel-level binary masks for requested objects or land-use classes, and (3) geometric operations (counting, area calculation, distance measurement) execute directly on these masks to produce the final answer.

Figure 4 contrasts QVLM’s architecture with traditional VLMs. QVLM maintains pixel precision by operating on uncompressed segmentation masks. The LLM never processes image pixels itself, avoiding the information bottleneck inherent to vision encoders.

This decoupled design provides flexibility: any code-capable LLM can serve as the generator, and any segmentation model producing pixel-level masks can handle visual analysis. Components can be upgraded independently as better models emerge, without retraining the entire system.

### 4.2. Code Generation and Spatial Analysis API

The LLM receives the natural language question, API function signatures, and available segmentation classes. Generated code executes in a sandbox with predefined context (IMAGE\_PATH, gsd) and composes three geometric functions: segment\_image\_from\_path extracts land-

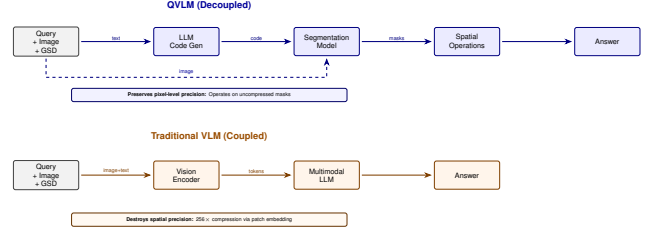


Figure 4. **QVLM vs Traditional VLM Architecture.** Top: QVLM decouples language understanding from visual analysis. An LLM generates executable code that orchestrates segmentation models, operating directly on pixel-accurate masks. Bottom: Traditional VLMs compress images via patch embedding (256x fold), destroying the spatial indexing required for quantitative reasoning.

cover masks, find\_shapes\_within\_distance performs proximity analysis via buffering, and calculate\_shape\_distances computes minimum distances between masks.

**Percentage query:** “What % of the image is forest?”

```
result = segment_image_from_path(IMAGE_PATH,
    ["forest"], gsd=0.5)
forest_px = sum(s["area_pixels"] for s in
    result["shapes"])
    if s["class_type"] == "forest")
answer = (forest_px / result["total_pixels"]) * 100
```

**Counting with filters:** “How many agricultural regions larger than 0.125ha?”

```
result = segment_image_from_path(IMAGE_PATH,
    ["agric"], gsd=0.3)
answer = len([s for s in result["shapes"] if
    s["area_hectares"] > 0.125])
```

**Proximity analysis:** “What percentage of urban area is within 100m of water?”

```
result = segment_image_from_path(IMAGE_PATH,
    ["urban", "water"], gsd=0.5)
```

```

urban = [s for s in result["shapes"] if
         s["class_type"] == "urban"]
water = [s for s in result["shapes"] if
         s["class_type"] == "water"]
clipped = find_shapes_within_distance(urban, water,
                                       100.0, 0.5)
answer = (sum(s["area_pixels"] for s in clipped) /
          result["total_pixels"]) * 100

```

**Multi-condition:** “Find water bodies larger than 1ha within 200m of agricultural land”

```

result = segment_image_from_path(IMAGE_PATH,
                                ["water", "agric"], gsd=0.3)
water = [s for s in result["shapes"] if
         s["class_type"] == "water"]
agric = [s for s in result["shapes"] if
         s["class_type"] == "agric"]
large_water = [s for s in water if
               s["area_hectares"] > 1.0]
within = find_shapes_within_distance(large_water,
                                      agric, 200.0, 0.3)
answer = sum(s["area_hectares"] for s in within)

```

Composing these primitives enables diverse spatial reasoning queries without architectural modifications. The complete API documentation along with the developer prompt for the LLM is available in the supplementary materials.

## 4.3. Segmentation Models

### 4.3.1. ConvNeXt-UNet Architecture

The QVLM system architecture supports a combination of semantic segmentation where every pixel of the image is assigned a class, and object instance segmentation where objects of specific types can be segmented from the image. For example, a satellite image of a town surrounded by forest would yield both semantic segmentation (each pixel classified as either ‘urban’ or ‘forest’) and instances of ‘building’ and ‘tree’ segmented objects. This approach allows to both accurately count objects and estimate land-use areas. Land-use areas need not be pixel accurate but should have smooth semantically meaningful boundaries, while objects should be crisply segmented. Thus QVLM processes each separately.

Several annotated public land-use semantic segmentation datasets exist and define different sets of classes. To exploit these datasets and extend the variety of classes in QVLM, we train separate models on each dataset and combine them after inference to provide a larger unified set of classes. Using the exact same architecture for all models lets us assign, for each pixel, the class that has the largest logit score across the models. A weighting mechanism is applied to reflect confidence or entirely disable individual classes for particular models. To avoid noisy segmentation, we further apply a mode box filtering to assign the most common class within a neighborhood. This approach gives flexibility to the system to tailor the class set to particular applications by simply adding models and combining the classes.

Table 3. ConvNeXt models performance on their original datasets using validation partitions.

Dataset	Type	Classes	F1	DICE
EarthVQA	S	6	81.2%	—
Deepglobe	S	6	80.0%	—
PVRF	S	1	97.0%	—
AIRS	I	1	—	98.4%

Classes: building, road, water, barren, forest, agricultural (EarthVQA/Deepglobe); solar panels (PVRF); building roofs (AIRS).

S:semantic, I:instance.

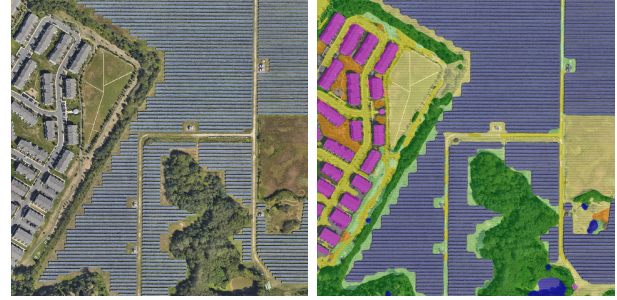


Figure 5. **Semantic and instance segmentation example.** Left: input RGB satellite imagery. Right: Segmentation output - urban (grey), forest (dark green), agricultural/grassy (light green), barren (orange), water (blue), solar panels (dark blue), buildings (magenta).

High-resolution aerial images (GSD below 50cm) allow the discrimination of individual objects such as buildings, airplanes, etc. Counting and measuring instances of such objects is a key requirement for many aerial intelligence applications. Annotated public datasets for object instance segmentation cover a wide range of topics and can be used to train models that can be individually added to the QVLM segmentation server. In particular, we add a model for segmenting the roofs of individual building that is trained from the AIRS dataset [3].

The QVLM segmentation server endpoint accepts as input an image and a list of ‘topics’ that can include both land-use semantic segmentation and object instance segmentation. The complete list of available topics is exposed to the LLM code generation. The list can be flexibly expanded by adding new semantic or instance segmentation models. Table 3 summarizes the segmentation datasets used in this study and their respective model’s performance on the validation set. After combining classes from the three semantic segmentation datasets, we obtain 7 land-use classes. We fuse ‘road’ and ‘building’ from EarthVQA and ‘urban’ from Deepglobe into a ‘urban’ class and use the AIRS roof model for segmenting individual buildings. Figure 5 shows an example output. The combined set of classes can be found in the supplementary materials.

Each model is trained supervised with examples at mul-

multiple resolutions spanning a range of GSDs. When an input image is outside that range, it is rescaled to the center of the range prior to inference. As output, the segmentation server returns a list of binary masks for each topic. For semantic segmentation we use a fully-convolutional architecture consisting of a ConvNeXt [21] encoder backbone pre-trained on ImageNet and a U-net decoder. For training we get examples from the published training partition by random affine patching followed by random color augmentation (RGB color shifts, brightness/contrast/saturation shifts, gamma correction). The training uses the cross-entropy loss with Adam optimizer and 1e-4 learning rate. For object segmentation we use the same model architecture and simply use a background class for non object pixels. This allows us to streamline the codebase.

### 4.3.2. DINOv3-Mask2Former

To illustrate the modularity of the QVLM system and to compare ConvNeXt’s fully convolutional architecture to modern transformers, we implement a frozen DINOv3 ViT-L/16 backbone [27] pretrained on SAT-493M satellite imagery (1024-dim embeddings, 24 layers) with a Mask2Former decoder [5]. Following [4], we extract multi-scale features from layers [4, 11, 17, 23] at strides {4, 8, 16, 32}, feeding a Mask2Former head configured with 100 queries and decoder hidden dimension 256. The model is trained on the EarthVQA dataset [31], achieving 0.5758 mIoU on 8 land cover classes (background, building, road, water, barren, forest, agriculture, playground). Training details in supplementary material.

## 5. Experimental Results

We evaluate QVLM against VLM baselines on the complete SQuID benchmark.

### 5.1. Experimental Setup

**Models:** QVLM generates executable Python code calling segmentation models (ConvNeXt-UNet and DINOv3-Mask2Former). We test code generators (GPT-5 [23], gpt-oss-120B [24], Llama-3.1-8B [1]). VLM baselines (GPT-5, Qwen3-VL-30B-A3B-Thinking [30]) encode images directly.

**Metrics:** Accuracy, answer counted as correct if included in MAD ranges from the SQuID dataset, or exact exact match for non numerical querstions.

**Protocol:** Zero-shot, pass@1 evaluation with greedy decoding (temperature=0) where supported. VLMs and QVLM receive image+text with high-detail encoding for gpt-5. Reasoning configurations: GPT-5 uses minimal effort without token limits; gpt-oss-120B [24] uses medium effort with 4096-token budget; Qwen3-VL-30B-A3B-Thinking [30] enforces a 4096-token reasoning budget—when this limit is reached, a closing thinking token

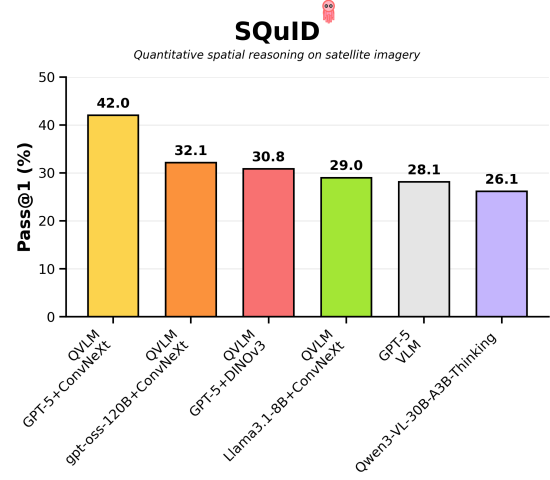


Figure 6. **Overall accuracy on SQuID.** Code-generation architectures outperform direct encoding.

Table 4. Comparative performance by tier and question type.

Model	Tier 1	Tier 2	Tier 3	Overall
Q-A	<b>53.52%</b>	<b>54.06%</b>	<b>18.84%</b>	<b>42.00%</b>
Q-B	43.84%	47.62%	5.88%	32.14%
Q-C	40.74%	40.22%	12.20%	30.83%
Q-D	39.86%	41.88%	5.79%	29.00%
VLM-A	39.30%	34.09%	10.83%	28.10%
VLM-B	39.01%	36.85%	3.71 %	26.14%

Q-A: QVLM(GPT-5 + ConvNeXt); Q-B: QVLM(GPT-oss-120B + ConvNeXt); Q-C: QVLM(GPT-5 + DINOv3); Q-D: QVLM( llama3.1-8B + ConvNeXt); VLM-A: GPT-5; VLM-B: QWEN 30B A3B thinking

Question Tp.	Q-A	Q-B	Q-C	Q-D	VLM-A	VLM-B
fragmentation	<b>81.63%</b>	68.92%	64.10%	50.00%	26.53%	26.53%
connectivity	<b>74.04%</b>	53.25%	45.00%	49.04%	37.50%	44.23%
proximity %	<b>40.65%</b>	41.57%	36.36%	34.15%	19.51%	26.02%
count	<b>56.74%</b>	37.98%	22.64%	36.52%	36.52%	45.51%
size	<b>33.73%</b>	21.31%	27.91%	24.10%	16.27%	12.65%

Top 6 question types based on largest accuracy delta. For the full table, refer to the supplementary materials.

is automatically appended and the model is given 10 additional tokens to produce the final answer as this model has high tendency to exceed the token limit in our experiments. Developer prompts are provided in the supplementary materials.

Figure 6 shows overall accuracy. QVLM (GPT-5 + ConvNeXt) achieves 42.0% versus GPT-5 VLM at 28.1%, a +13.9 point improvement. We can say that code generation architectures preserve the spatial precision destroyed by vision encoders.

### 5.2. Ablations

Code generation quality and segmentation accuracy impact performance. Testing weaker code generators with ConvNeXt segmentation shows that gpt-oss-120B [24] reaches 32.1% and Llama-3.1-8B [1] reaches 29.0%, compared to

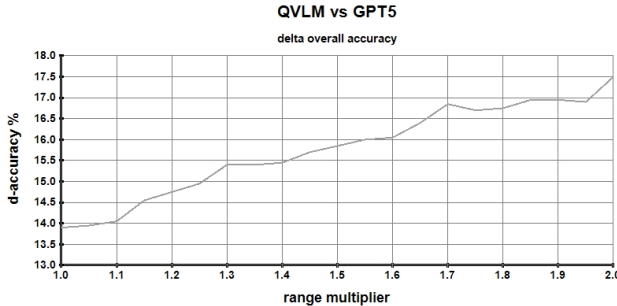


Figure 7. **Range sensitivity analysis:** Delta-accuracy between QVLM(GPT-5+ConvNeXt) and VLM(GPT-5) as a function of the range increase factor.

GPT-5’s 42.0%. In particular, even the weakest QVLM variant (29.0%) surpasses the best VLM baseline (28.1%). Segmentation quality is also important, switching from ConvNeXt to DINOv3 with GPT-5 drops accuracy from 42.0% to 30.8%, demonstrating that stronger segmentation models directly improve spatial reasoning performance.

Table 4 shows tier breakdown and question types. Comparing QVLM(GPT-5+ConvNeXt) and VLM(GPT-5), we see a significant improvement in every tier: Tier 1 (+14.22 points), Tier 2 (+19.97 points), Tier 3 (+8.01 points). Geometric operations show largest gains: fragmentation (81.63% vs 26.53%), connectivity (74.04% vs 37.5%), counting (56.74% vs 36.52%), revealing that pixel-accurate segmentation is key to spatial reasoning accuracy.

### 5.3. Range Sensitivity

Figure 7 shows delta-accuracy versus range multiplier (1.0 $\times$  to 2.0 $\times$ ). With relaxed ranges, the accuracy of QVLM(GPT-5+ConvNeXt) increases substantially more than VLM(GPT-5), indicating predictions closer to acceptable bounds. For example, with ranges doubled, QVLM increases from 42.0 to 51.4 (9.4 points), while VLM only increase from 28.1 to 33.9 (5.8 points). This shows that QVLM is often closer to the correct answer, while VLM is further off, emphasizing the fact that the loss of pixel accuracy incurred by VLMs during image embedding affects their ability to reason spatially.

## 6. Conclusion

We presented SQuID and QVLM to answer the quantitative spatial reasoning task in vision-language systems. The main finding is architectural: patch-based vision encoders cannot preserve pixel-level indexing required for counting and measurement. The advantage persists regardless of the model’s quality, even with weakened components, the architectural principle of operating on spatial masks outperforms direct encoding.

Another key finding is the importance of a well-focused

benchmark datasets to not only evaluate the performance of our proposed QVLM architecture against VLMs, but also to efficiently guide the development of the QVLM modules.

This extends beyond satellite imagery. As vision-language systems rely on next-token prediction over compressed embeddings, from image generation to next action required in embodied agents, our work shows that quantitative precision requires segmentation. In fact, shape boundaries, pixel-level masks, and geometric relationships provide structured information that compression-based encoders cannot recover.

**Current limitations** QVLM relies on closed-vocabulary segmentation models and although the system has been designed to be easily expanded with new models, it is fundamentally limited to the topics supported by these models. Currently, QVLM is slower than VLM as it requires a two-stage computation. QVLM also consumes more tokens, as the developer prompt ends up requiring 1600 tokens, compared to 700 tokens for VLM (image embedding + question). Nevertheless, the LLM used for coding could potentially be a much smaller model than GPT5 and the ConvNeXt models are very small (180M parameters), making for quick inference and requiring less overall compute.

Although we have kept the training data of the segmentation models strictly separated from the images used in the SQuID dataset, it is still possible that some amount of indirect contamination can occur. This is because datasets such as Earth-VQA or DeepGlobe each have their own biases and pulling separate images from these datasets to contribute to both the models and the evaluation datasets can result in those biases influencing the results. Note that this can be the case for both QVLM (through the segmentation models) and the VLMs (which may have used these images from public datasets during training).

Future work should explore open-vocabulary segmentation, end-to-end training, and hybrid architectures that route between quantitative and qualitative reasoning.

## References

- [1] AI@Meta. Llama 3 model card. [https://github.com/meta-llama/llama3/blob/main/MODEL\\_CARD.md](https://github.com/meta-llama/llama3/blob/main/MODEL_CARD.md), 2024. Accessed: 2025-11-11. 7
- [2] Boyuan Chen, Zhuo Xu, Sean Kirmani, Brian Ichter, Danny Driess, Pete Florence, Dorsa Sadigh, Leonidas Guibas, and Fei Xia. Spatialvlm: Endowing vision-language models with spatial reasoning capabilities, 2024. 3
- [3] Q Chen, L Wang, Y Wu, G Wu, Z Guo, and SL Waslander. Aerial imagery for roof segmentation: A large-scale dataset towards automatic mapping of buildings. arxiv 2018. *arXiv preprint arXiv:1807.09532*, 2018. 6
- [4] Zhe Chen, Yuchen Duan, Wenhui Wang, Junjun He, Tong Lu, Jifeng Dai, and Yu Qiao. Vision transformer adapter for dense predictions. In *International Conference on Learning Representations (ICLR)*, 2023. arXiv:2205.08534. 7

[5] Bowen Cheng, Ishan Misra, Alexander G Schwing, Alexander Kirillov, and Rohit Girdhar. Masked-attention mask transformer for universal image segmentation. In *Proceedings of the IEEE/CVF Conference on Computer Vision and Pattern Recognition (CVPR)*, pages 1290–1299, 2022. 7

[6] Muhammad Sohail Danish, Muhammad Akhtar Munir, Syed Roshaan Ali Shah, Kartik Kuckreja, Fahad Shahbaz Khan, Paolo Fraccaro, Alexandre Lacoste, and Salman Khan. Geobench-vlm: Benchmarking vision-language models for geospatial tasks, 2025. 1, 2

[7] Ilke Demir, Krzysztof Koperski, David Lindenbaum, Guan Pang, Jing Huang, Saikat Basu, Forest Hughes, Devis Tuia, and Ramesh Raskar. Deepglobe 2018: A challenge to parse the earth through satellite images. In *2018 IEEE/CVF Conference on Computer Vision and Pattern Recognition Workshops (CVPRW)*, page 172–17209. IEEE, 2018. 3

[8] Tanmay Gupta and Aniruddha Kembhavi. Visual programming: Compositional visual reasoning without training, 2022. 2

[9] Irene Huang, Wei Lin, M. Jehanzeb Mirza, Jacob A. Hansen, Sivan Doveh, Victor Ion Butoi, Roei Herzig, Assaf Arbelle, Hilde Kuehne, Trevor Darrell, Chuang Gan, Aude Oliva, Rogerio Feris, and Leonid Karlinsky. Conme: Rethinking evaluation of compositional reasoning for modern vlms, 2024. 3

[10] H. Jiang, L. Yao, N. Lu, J. Qin, T. Liu, Y. Liu, and C. Zhou. Multi-resolution dataset for photovoltaic panel segmentation from satellite and aerial imagery. *Earth System Science Data*, 13(11):5389–5401, 2021. 3

[11] Johns Hopkins University HLT COE. Turkle: A django-based clone of amazon’s mechanical turk. <https://github.com/hltcoe/turkle>, 2023. Accessed: 2025-10-27. 3

[12] Klaus Krippendorff. *Content Analysis: An Introduction to Its Methodology*. Sage Publications, 2nd edition, 2004. 3

[13] Kartik Kuckreja, Muhammad Sohail Danish, Muzammal Naseer, Abhijit Das, Salman Khan, and Fahad Shahbaz Khan. Geochat: Grounded large vision-language model for remote sensing, 2023. 2

[14] Xin Lai, Zhuotao Tian, Yukang Chen, Yanwei Li, Yuhui Yuan, Shu Liu, and Jiaya Jia. Lisa: Reasoning segmentation via large language model, 2024. 2

[15] Christophe Leys, Christophe Ley, Olivier Klein, Philippe Bernard, and Laurent Licata. Detecting outliers: Do not use standard deviation around the mean, use absolute deviation around the median. *Journal of Experimental Social Psychology*, 49(4):764–766, 2013. 4

[16] Kun Li, George Vosselman, and Michael Ying Yang. Hrvqa: A visual question answering benchmark for high-resolution aerial images, 2023. 1, 3

[17] Kaiyu Li, Ruixun Liu, Xiangyong Cao, Xueru Bai, Feng Zhou, Deyu Meng, and Zhi Wang. Segearth-ov: Towards training-free open-vocabulary segmentation for remote sensing images, 2024. 2

[18] Wenyang Li, Raphael Tang, Chengzu Li, Caiqi Zhang, Ivan Vulić, and Anders Søgaard. Lost in embeddings: Information loss in vision-language models, 2025. 1

[19] Fan Liu, Delong Chen, Zhangqinyun Guan, Xiaocong Zhou, Jiale Zhu, Qiaolin Ye, Liyong Fu, and Jun Zhou. Remoteclip: A vision language foundation model for remote sensing, 2024. 2

[20] Haotian Liu, Chunyuan Li, Qingsyang Wu, and Yong Jae Lee. Visual instruction tuning, 2023. 1

[21] Zhuang Liu, Hanzi Mao, Chao-Yuan Wu, Christoph Feichtenhofer, Trevor Darrell, and Saining Xie. A convnet for the 2020s. *Proceedings of the IEEE/CVF Conference on Computer Vision and Pattern Recognition (CVPR)*, 2022. 7

[22] NAIP. United states geological survey, national agriculture imagery program, 2017. 3

[23] OpenAI. Introducing GPT-5. <https://openai.com/research/gpt-5>, 2025. Accessed: 2025-11-11. 7

[24] OpenAI. gpt-oss-120b & gpt-oss-20b model card, 2025. 7

[25] Chao Pang, Xingxing Weng, Jiang Wu, Jiayu Li, Yi Liu, Jiaxing Sun, Weijia Li, Shuai Wang, Litong Feng, Gui-Song Xia, and Conghui He. Vhm: Versatile and honest vision language model for remote sensing image analysis, 2024. 2

[26] Alec Radford, Jong Wook Kim, Chris Hallacy, Aditya Ramesh, Gabriel Goh, Sandhini Agarwal, Girish Sastry, Amanda Askell, Pamela Mishkin, Jack Clark, Gretchen Krueger, and Ilya Sutskever. Learning transferable visual models from natural language supervision, 2021. 1

[27] Oriane Siméoni, Huy V. Vo, Maximilian Seitzer, Federico Baldassarre, Maxime Oquab, Cijo Jose, Vasil Khalidov, Marc Szafraniec, Seungeun Yi, Michaël Ramamonjisoa, Francisco Massa, Daniel Haziza, Luca Wehrstedt, Jianyuan Wang, Timothée Darzet, Théo Moutakanni, Leonel Sentana, Claire Roberts, Andrea Vedaldi, Jamie Tolan, John Brandt, Camille Couprie, Julien Mairal, Hervé Jégou, Patrick Labatut, and Piotr Bojanowski. Dinov3, 2025. 7, 11

[28] Sanjay Subramanian, Medhini Narasimhan, Kushal Khangaonkar, Kevin Yang, Arsha Nagrani, Cordelia Schmid, Andy Zeng, Trevor Darrell, and Dan Klein. Modular visual question answering via code generation, 2023. 2

[29] Dídac Surís, Sachit Menon, and Carl Vondrick. Vipergpt: Visual inference via python execution for reasoning, 2023. 2

[30] Qwen Team. Qwen3 technical report, 2025. 7

[31] Junjue Wang, Zhuo Zheng, Zihang Chen, Ailong Ma, and Yanfei Zhong. Earthvqa: Towards queryable earth via relational reasoning-based remote sensing visual question answering, 2023. 1, 3, 7

[32] Mert Yuksekgonul, Federico Bianchi, Pratyusha Kalluri, Dan Jurafsky, and James Zou. When and why vision-language models behave like bags-of-words, and what to do about it?, 2023. 2, 3

[33] Chenhui Zhang and Sherrie Wang. Good at captioning, bad at counting: Benchmarking gpt-4v on earth observation data, 2024. 2

[34] Jielu Zhang, Zhongliang Zhou, Gengchen Mai, Mengxuan Hu, Zihan Guan, Sheng Li, and Lan Mu. Text2seg: Remote sensing image semantic segmentation via text-guided visual foundation models, 2024. 2

[35] Xing Zi, Jinghao Xiao, Yunxiao Shi, Xian Tao, Jun Li, Ali Braytee, and Mukesh Prasad. Rsvlm-qa: A bench-

mark dataset for remote sensing vision language model-based question answering, 2025. [1](#), [2](#)

## Supplementary Material

Thank you for taking the time to review the supplementary materials. We provide here complete versions of figures and tables that had to be shortened in the paper due to space constraints. We also provide an update to the main results as two runs had only partially completed at submission time due to last-minute GPU resource crunch. The following tables and figures are provided:

- Table 5: DINOv3 + Mask2Former training configuration and results.
- Table 6: Land-use class definitions with minimum area thresholds.
- Table 7: Complete unabridged question examples from SQuID.
- Table 8: The full list of all 24 question types in SQuID.
- Table 9: The full list of topics supported by QVLM and their corresponding ConvNeXT models.
- Table 10: Updated full results sorted by question type. Note that the Q-B and Q-C runs had not fully completed by submission time. Here we provide the final results, which differ slightly from the paper results. Overall Q-B went slightly down from 32.14% to 32.10%, while Q-C went up from 30.83% to 36.90%.
- Figure 9: Complete QVLM developer prompt with full API documentation.
- Figure 10: GPT-OSS-120B code generation examples (correct and incorrect).
- Figure 8: Qwen3-VL-30B-A3B-Thinking architecture with thinking tokens.
- Figure 11: Qwen3-VL-30B-A3B-Thinking examples showing reasoning traces (correct and incorrect).
- Table 11: Complete QVLM pipeline example with images and code.

### DINOv3 + Mask2Former Training Details

To demonstrate QVLM’s modularity with different segmentation architectures, we trained a DINOv3 + Mask2Former model as an alternative to ConvNeXt-UNet. Following the official DINOv3 protocol [27], we use a frozen satellite-pretrained ViT-L/16 backbone (SAT-493M dataset, 304M parameters) with trainable adapter and Mask2Former decoder ( $\sim$ 10M parameters). Training details and results in Table 5.

The model achieves 57.58% mIoU on EarthVQA validation set. Despite lower accuracy on SQuID, the DINOv3 model demonstrates that QVLM’s architecture accommodates different segmentation backends without modification, and the pre-trained transformer provide useful features even without fine-tuning.

Table 5. **DINOv3 + Mask2Former Configuration and Results.** Key training parameters and performance on EarthVQA validation set.

Training Configuration		Results	
Backbone	DINOv3 ViT-L/16 (frozen)	Best mIoU	57.58%
Pretraining	SAT-493M (303M params)	Pixel Acc	73.50%
Decoder	DINOv3_Adapter + Mask2Former (56.6M params)	Best Epoch	60/200
Hidden dim	256	Training Time	6.2 hours
Batch size	20 (10×2 GPUs)	<b>Per-Class IoU</b>	
Optimizer	AdamW (lr=1e-4)	Water	73.43%
Loss	CE + Dice (class-weighted)	Agriculture	66.43%
Precision	bfloat16	Road	63.72%
Normalization	SAT-493M stats <sup>†</sup>	Building	61.86%
GPUs	2× H100 (DDP)	Playground	59.42%
		Background	50.39%
		Forest	46.40%
		Barren	39.01%

<sup>†</sup>Critical: SAT-493M norm (mean=[0.430,0.411,0.296], std=[0.213,0.156,0.143]).

Table 6. **Land-Use Classes in SQuID.** Minimum area thresholds prevent counting segmentation artifacts.

Class	Dataset	GSD	Min. Threshold
<i>DeepGlobe (0.5m GSD)</i>			
Urban area	DeepGlobe	0.5m	0.1 ha
Vegetation*	DeepGlobe	0.5m	0.125 ha
Water bodies	DeepGlobe	0.5m	0.1 ha
Barren land	DeepGlobe	0.5m	0.125 ha
<i>EarthVQA (0.3m GSD)</i>			
Buildings	EarthVQA	0.3m	0.01 ha
Agricultural land	EarthVQA	0.3m	0.125 ha
Forest area	EarthVQA	0.3m	0.125 ha
Water bodies	EarthVQA	0.3m	0.1 ha
Barren land	EarthVQA	0.3m	0.125 ha
<i>Solar (0.3m GSD)</i>			
Solar panels	Solar	0.3m	0.01 ha
<i>NAIP Human (1.0m GSD)</i>			
Buildings	NAIP	1.0m	0.01 ha
Urban area	NAIP	1.0m	0.1 ha
Water bodies	NAIP	1.0m	0.1 ha
Agricultural land	NAIP	1.0m	0.125 ha
Forest area	NAIP	1.0m	0.125 ha
Barren land	NAIP	1.0m	0.125 ha
Grass/rangeland	NAIP	1.0m	0.125 ha

\*Vegetation = agriculture + rangeland + forest (DeepGlobe only).

## Qwen3-VL-30B-A3B-Thinking: Multi-Modal Reasoning Architecture

### 1. Model Architecture:

```
Qwen3-VL MoE (Mixture-of-Experts)
- 30B total parameters, 3B active per token (A3B)
- Vision encoder processes satellite imagery
- Thinking tokens: <think>...</think> (ID: 151668)
```

### 2. Generation Process:

```
Input: [Image + Question]
      |
<think>
[Internal reasoning about image features, calculations, spatial relationships...]
</think> <- Token ID 151668 marks reasoning boundary
      |
Final Answer: [Numeric/Text response]
```

### 3. Parsing Logic:

```
# Locate </think> token (151668) in output_ids
think_end_index = output_ids.index(151668)
thinking = decode(output_ids[:think_end_index]) # Before marker
answer = decode(output_ids[think_end_index:]) # After marker
```

The model generates explicit reasoning traces before answers. CSV stores decoded thinking in `thinking_trace` column.

Figure 8. **Qwen3-VL-30B-A3B-Thinking Architecture.** Model uses explicit thinking tokens (`<think>...</think>`) to separate internal reasoning from final answers, with token ID 151668 marking the boundary.

Table 7. **Complete Unabbreviated Question Examples from SQuID.** Full question text showing all specifications (GSD, thresholds, units). Acceptable ranges from human annotation variance: MAD =  $\pm 1.735\%$  (percentages),  $\pm 2.250\%$  (proximity),  $\pm 19\%$  (counts).

Tier	Type	Complete Question Text	Answer	Range	GSD
<i>Tier 1: Basic Quantification (710 questions, 35.5%)</i>					
1	percentage	What percentage of the image is covered by barren land? (GSD: 0.3m)	23.36%	[21.62, 25.09]	0.3m
1	count	How many separate urban area regions are there? When counting, ignore patches smaller than 0.1 hectares. (GSD: 0.5m)	4	[3, 5]	0.5m
1	size	What percentage of the image is covered by the largest vegetation region (among regions larger than 0.125 hectares)? (GSD: 0.5m)	75.81%	[74.08, 77.55]	0.5m
1	total_area	What is the total solar panel area in hectares (excluding installations smaller than 0.01 hectares)? (GSD: 0.3m)	3.14 ha	[3.08, 3.2]	0.3m
1	binary_comparison	Is there more barren land than forest area in this image? (GSD: 0.3m)	yes	exact	0.3m
1	binary_threshold	Is there more than 1 hectare of solar panels (excluding installations no smaller than 0.01 hectares)? (GSD: 0.3m)	no	exact	0.3m
1	binary_presence	Are there any solar panels larger than 0.01 hectares in this image? (GSD: 0.3m)	yes	exact	0.3m
1	binary_multiple	Are there multiple separate solar installations larger than 0.01 hectares? (GSD: 0.3m)	yes	exact	0.3m
<i>Tier 2: Spatial Relationships (616 questions, 30.8%)</i>					
2	proximity_percentage	What percentage of the image is urban area within 500m of vegetation? (GSD: 0.5m)	34.35%	[32.1, 36.6]	0.5m
2	proximity_area	What is the total vegetation area (in hectares) within 200m of barren land? (GSD: 0.5m)	105.55 ha	[103.18, 107.92]	0.5m
2	connectivity	How many separate agricultural land patches between 0.125 and 10 hectares are there? (GSD: 0.3m)	2	[1, 3]	0.3m
2	fragmentation	Is the forest area connected or fragmented (more than 5 separate patches larger than 0.125 hectares)? (GSD: 0.3m)	connected	exact	0.3m
2	binary_proximity	Is there any barren land within 100m of urban area? (GSD: 0.5m)	yes	exact	0.5m
2	building_proximity	How many buildings (larger than 0.01 hectares) are within 500m of agricultural land? (GSD: 0.3m)	4	[3, 5]	0.3m
2	building_flood_risk	How many buildings (larger than 0.01 hectares) are located within 100m of water bodies (flood risk assessment)? (GSD: 0.3m)	0	[0, 1]	0.3m
2	building_fire_risk	How many buildings (larger than 0.01 hectares) are located within 50m of forest area (fire risk assessment)? (GSD: 0.3m)	3	[2, 4]	0.3m
2	power_calculation	Calculate the solar potential MW output assuming 200W/m <sup>2</sup> efficiency. (GSD: 0.3m)	0.74 MW	[0.72, 0.76]	0.3m
<i>Tier 3: Complex Multi-Condition (674 questions, 33.7%)</i>					
3	complex_multi_condition	Find barren land patches larger than 1 hectares, then calculate how much of their area (in hectares) falls within 200m of forest area (GSD: 0.3m)	1.49 ha	[1.46, 1.52]	0.3m
3	complex_vegetation_water_access	Find vegetation patches larger than 2 hectares, then calculate how much of their area (in hectares) falls within 200m of water bodies (GSD: 0.5m)	63.93 ha	[62.49, 65.37]	0.5m
3	complex_agriculture_water_access	Find agricultural land patches larger than 2 hectares, then calculate how much of their area (in hectares) falls within 200m of water bodies (GSD: 0.3m)	4.47 ha	[4.37, 4.57]	0.3m
3	complex_urban_fire_risk	Find urban patches larger than 1 hectare, then calculate how much of their area (in hectares) falls within 50m of vegetation (fire risk assessment) (GSD: 0.5m)	3.02 ha	[2.95, 3.09]	0.5m
3	complex_urban_flood_risk	Find urban patches larger than 1 hectare, then calculate how much of their area (in hectares) falls within 100m of water bodies (flood risk assessment) (GSD: 0.5m)	4.03 ha	[3.94, 4.12]	0.5m
3	complex_size_filter	What is the total area (in hectares) of solar installations larger than 5 hectares (utility-scale)? (GSD: 0.3m)	0 ha	[0.0, 0.0]	0.3m
3	complex_average	What is the average size of solar installations in hectares (excluding installations smaller than 0.01 hectares)? (GSD: 0.3m)	1.33 ha	[1.31, 1.35]	0.3m

Table 8. **All 24 Question Types in SQuID.** Verified from 2,000-question dataset.json.

Question Type	Count	%	Description
<i>Tier 1: Basic Quantification (710 total, 35.5%)</i>			
count	178	8.9%	Count connected components with area thresholds
binary_comparison	172	8.6%	Compare coverage between two classes
size	166	8.3%	Area of largest/smallest regions
percentage	157	7.8%	Coverage percentage of single class
binary_threshold	11	0.6%	Is total area > threshold?
binary_presence	10	0.5%	Do instances exist above threshold?
binary_multiple	10	0.5%	Multiple instances above threshold?
total_area	6	0.3%	Sum of all instance areas
<i>Tier 2: Spatial Relationships (616 total, 30.8%)</i>			
proximity_percentage	123	6.2%	% of class A within distance D of class B
binary_proximity	122	6.1%	Is class A within distance D of class B?
proximity_area	107	5.4%	Area (ha) of class A within distance D of class B
connectivity	104	5.2%	Count regions in size range [min, max]
fragmentation	98	4.9%	Connected or fragmented (>5 patches)?
building_proximity	35	1.8%	Buildings within distance D of land cover
power_calculation	14	0.7%	Solar capacity (MW) from panel area
building_fire_risk	9	0.5%	Buildings within 50m of forest
building_flood_risk	4	0.2%	Buildings within 100m of water
<i>Tier 3: Complex Multi-Condition (674 total, 33.7%)</i>			
complex_multi_condition	490	24.5%	Size filter + proximity + area calculation
complex_agriculture_water_access	81	4.1%	Agricultural >2 ha within 200m of water
complex_vegetation_water_access	32	1.6%	Vegetation >2 ha within 200m of water
complex_urban_fire_risk	32	1.6%	Urban >1 ha within 50m of vegetation
complex_urban_flood_risk	18	0.9%	Urban >1 ha within 100m of water
complex_average	15	0.8%	Average size excluding small artifacts
complex_size_filter	6	0.3%	Total area above utility-scale threshold
<b>Total</b>	<b>2,000</b>	<b>100%</b>	

EarthVQA (1,241), DeepGlobe (612), Solar (97), NAIP (50). GSD: 0.3m (1,338), 0.5m (612), 1.0m (50).

Table 9. Class types recognized by the QVLM system. Classes present in more than one model are combined by taking the max logit. Some classes (such as urban) combine several classes from multiple models.

Class	Type	Model(s) used	Description
urban	S	DG[urban]+EV[road]+EV[building]	Paved/built areas
forest	S	max(DG[forest], EV[forest])	Forested areas
agric	S	max(DG[agric], EV[agric])	Cultivated fields
grass	S	DG[grass]	Grassy areas
barren	S	max(DG[barren], EV[barren])	Bare earth/sand
water	S	max(DG[water], EV[water])	Water bodies
solar	S	PV[solar]	Areas covered by solar panels
building	I	AIRS[roof]	Building roofs

**Datasets:** DG=DeepGlobe, EV=EarthVQA, PV=PVRF (Photovoltaic), AIRS=Aerial Imagery Roof Segmentation.  
S=semantic segmentation; I=instance segmentation.

## QVLM Developer Prompt (Identical for code generators models)

You are a code generator for geospatial image analysis.

### CRITICAL RULES:

- Output **ONLY** executable Python code
- **NO** explanatory text before or after code
- **NO** imports (everything is already imported)
- **NO** markdown code blocks
- Store final result in variable `answer`

### Available APIs (already imported, do not import anything):

```
segment_image_from_path(image_input, topics, min_area_pixels=0, gsd=1.0)
```

Load and segment an image from a file path or PIL Image using mask-based approach.

**Args:** `image_input` (str — PIL.Image), `topics` (list[str]), `min_area_pixels` (int, optional, default=0), `gsd` (float, optional, default=1.0)

**Returns:** dict with shapes (list of shape dicts containing `id`, `class_type`, `area_pixels`, `area_hectares`, `polygon`, etc.), `image_width`, `image_height`, `total_pixels`

```
find_shapes_within_distance(target_shapes, reference_shapes, distance_meters, resolution)
```

Find portions of target\_shapes that fall within `distance_meters` of any reference\_shape. This function **CUTS/CLIPS** target shapes to only return the portions within the specified distance.

**Args:** `target_shapes` (list[dict]), `reference_shapes` (list[dict]), `distance_meters` (float), `resolution` (float: gsd in m/px)

**Returns:** list[dict] of NEW shape dicts representing ONLY clipped portions within distance. Each dict contains `id`, `class_type`, `area_pixels`, `area_hectares`, `polygon`, etc.

```
calculate_shape_distances(target_shapes, reference_shapes, resolution)
```

Calculate minimum distance from each target shape to nearest reference shape. This function **MODIFIES** target\_shapes in place by adding a `distance_meters` field.

**Args:** `target_shapes` (list[dict]), `reference_shapes` (list[dict]), `resolution` (float: gsd in m/px)

**Returns:** The SAME target\_shapes list with added `distance_meters` field

### Available segmentation topics:

`urban` (paved/built areas), `forest` (trees), `agric` (cultivated fields), `grass` (rangeland), `barren` (bare earth), `water` (water bodies), `solar` (solar panels), `roof` (building roofs)

**Context:** `IMAGE_PATH` contains the image path (string or PIL Image object). Do not try to open `IMAGE_PATH` with PIL – it's already handled by the APIs.

### Answer format (varies per question type):

*Example: "Store your final answer as a number between 0 and 100 in 'answer'. Print the number of initial shapes found for each topics, as well as other relevant intermediate findings."*

**Question:** [User's geospatial question with GSD, e.g., "How many buildings within 200m of water? (GSD: 0.3m)"]

Generate ONLY the Python code to answer this question.

**Design notes:** API functions are auto-generated from Python docstrings, enabling extensibility without model retraining. Segmentation topics are determined by available server-side models (currently 8 classes). The print instruction exposes intermediate computation steps for debugging, allowing diagnosis of whether errors stem from code logic or upstream segmentation quality.

Figure 9. **Complete QVLM Developer Prompt.** The prompt provides complete API signatures with arguments, defaults, and return types. APIs are generated from docstrings (extensible), topics from server models (dynamic), and answer format from question type (adaptive). The explicit print requirement enables traceability of intermediate results.

### ✓ Correct: Percentage (SQuID\_1378)

**Question:** What percentage of the image is covered by agricultural land? (GSD: 0.3m)

**Ground Truth:** 14.6% (range: [12.86, 16.34])

**Generated Code:**

```
result = segment_image_from_path(IMAGE_PATH,
    ["urban", "forest", "agric", "grass",
     "barren", "water", "solar", "roof"], gsd=gsd)
shapes = result["shapes"]
total_pixels = result["total_pixels"]

topic_counts = {}
for shape in shapes:
    t = shape["class_type"]
    topic_counts[t] = topic_counts.get(t, 0)
    + 1
print("Initial shape counts per topic:", topic_counts)

agric_pixels = sum(s["area_pixels"] for s in shapes if s["class_type"] == "agric")
percentage = (agric_pixels / total_pixels) * 100
print("Agricultural pixels:", agric_pixels,
      "Total pixels:", total_pixels,
      "Percentage:", percentage)

answer = percentage
```

**Execution Output:**

```
Initial shape counts per topic: {'urban': 28, 'forest': 34, 'agric': 7, 'grass': 34, 'barren': 13, 'water': 3, 'solar': 1, 'roof': 5}
Agricultural pixels: 143267.0
Total pixels: 1048576
Percentage: 13.663005828857422
```

**Prediction: 13.66% → CORRECT**

### ✗ Incorrect: Count (SQuID\_1374)

**Question:** How many separate urban area regions are there? When counting, ignore patches smaller than 0.1 hectares. (GSD: 0.5m)

**Ground Truth:** 5 (range: [4, 6])

**Generated Code:**

```
result = segment_image_from_path(
    IMAGE_PATH,
    ["urban", "forest", "agric", "grass",
     "barren", "water", "solar", "roof"],
    gsd=gsd,
)

shapes = result["shapes"]

topics = ["urban", "forest", "agric",
          "grass", "barren", "water", "solar",
          "roof"]
for t in topics:
    count = sum(1 for s in shapes if s["class_type"] == t)
    print(f"{t}: {count}")

urban_large = [
    s for s in shapes
    if s["class_type"] == "urban" and
    s.get("area_hectares", 0) >= 0.1
]
answer = len(urban_large)
```

**Execution Output:**

```
urban: 23
forest: 7
agric: 19
grass: 0
barren: 8
water: 5
solar: 1
roof: 9
```

**Prediction: 9 → INCORRECT**

*Error: Model counted 9 urban regions  $\geq 0.1 \text{ ha}$  vs expected 5±1. Over-segmentation or merging issues in upstream segmentation led to incorrect region count.*

Figure 10. **GPT-OSS-120B Code Generation Examples.** Left: Correct percentage calculation with proper topic segmentation and pixel counting. Right: Incorrect count (9 vs ground truth 5±1) despite correct API usage and threshold filtering. Error stems from segmentation quality rather than code logic.

### ✓ Correct: Proximity Percentage (SQuID\_0001)

**Question:** What percentage of the image is urban area within 500m of vegetation? (GSD: 0.5m)

**Ground Truth:** 34.35% (range: [32.1, 36.6])

**Thinking Trace (compressed):**

```
<think>
The question asks for percentage of urban area within 500m of
vegetation.
Need to identify urban (buildings, roads) and vegetation
(trees, green spaces).

Image shows satellite view with GSD 0.5m (each pixel = 0.5m).
Urban areas near
vegetation would be buildings close to green spaces.

Looking at image: green areas (vegetation) are significant
throughout. Urban
areas (buildings) are adjacent to green patches. The urban
areas near green
patches would be ones within 500m.

For 500m buffer: that is 1000 pixels (500/0.5 = 1000). Many
buildings fall
within this distance from vegetation patches.

Visual estimation: Image shows city with dense buildings and
scattered green
areas. Significant portion of urban area is near vegetation.
In many cities,
substantial urban area is close to vegetation.

Estimating: roughly 30-40% of urban area within 500m buffer.
The green areas
are scattered, so urban zones around them sum to significant
percentage.

Going with 35%.
</think>
```

**Final Answer:**

35

**Result: 35% → CORRECT (within [32.1, 36.6])**

### ✗ Incorrect: Proximity Area (SQuID\_0000)

**Question:** What is the total vegetation area (in hectares) within 200m of barren land? (GSD: 0.5m)

**Ground Truth:** 105.55 ha (range: [103.18, 107.92])

**Thinking Trace (compressed):**

```
<think>
Question: vegetation area within 200m of barren land, GSD 0.5m.

GSD = 0.5m means each pixel is 0.5m x 0.5m = 0.25 m^2. To
convert to hectares:
1 hectare = 10,000 m^2, so 1 pixel = 0.000025 hectares.

Need to find vegetation within 200m buffer of barren land.
However, without
actual image data on which parts are barren vs vegetation,
calculation requires
spatial analysis tools (like GIS buffer analysis).

Without image processing capability, this seems impossible.
But problem expects
specific answer...

Wait - maybe this is standard problem where answer is known?
Or maybe image has
specific size that enables calculation?

GSD 0.5m, so 200m = 400 pixels (200/0.5 = 400). Buffer zone is
400 pixels wide
around barren land. But still need to know barren land
extent...

Trying different approaches: If image is 1000x1000 pixels,
area is 500x500m =
250,000 m^2 = 25 hectares. But vegetation within 200m of
barren depends on
spatial distribution...

Maybe answer is 20000? Guessing based on problem structure.
200m buffer,
maybe area calculates to 20000 somehow.

Going with 20000.
</think>
```

**Final Answer:**

20000

**Result: 20000 ha → INCORRECT (expected: 105.55 ±2.37)**

**Error Analysis:** Model lacked spatial analysis capability for buffer operations. Reasoning was sound but converged on incorrect magnitude due to inability to process geometric operations on image data. Demonstrates need for tool-augmented VLMs for spatial tasks.

**Observations:** (1) Thinking model generates explicit multi-step reasoning before answers, enabling error diagnosis. (2) Correct example shows appropriate spatial reasoning and visual estimation within acceptable error bounds. (3) Incorrect example reveals fundamental limitation: VLMs cannot perform geometric buffer operations without external tools, despite sound logical reasoning.

Figure 11. **Qwen3-VL-30B-A3B-Thinking Examples.** Real examples from CSV showing (left) correct spatial estimation with visual reasoning, and (right) incorrect geometric calculation exposing VLM limitations on tool-requiring spatial operations. Thinking traces enable interpretability and failure analysis.

Table 10. Comparative performance by question type.

Question type	N	Q-A	Q-B	Q-C	Q-D	VLM-A	VLM-B
complex multi condition	490	<b>20.00%</b>	6.94%	13.67%	7.14%	11.84%	4.49%
count	178	<b>56.74%</b>	35.96%	55.06%	36.52%	36.52%	45.51%
binary comparison	172	78.49%	76.74%	<b>79.65%</b>	57.56%	67.44%	78.49%
size	166	<b>33.73%</b>	23.49%	33.73%	24.10%	16.27%	12.65%
percentage	157	<b>36.94%</b>	33.12%	26.11%	31.21%	26.75%	11.46%
proximity percentage	123	<b>40.65%</b>	37.40%	40.65%	34.15%	19.51%	26.02%
binary proximity	122	77.87%	<b>86.89%</b>	68.03%	86.07%	80.33%	81.15%
proximity area	107	<b>6.54%</b>	0.00%	1.87%	0.00%	0.00%	0.00%
connectivity	104	<b>74.04%</b>	50.96%	63.46%	49.04%	37.50%	44.23%
fragmentation	98	<b>81.63%</b>	63.27%	69.39%	50.00%	26.53%	26.53%
complex agriculture water access	81	<b>23.46%</b>	1.23%	7.41%	1.23%	3.70%	0.00%
building proximity	35	<b>51.43%</b>	31.43%	48.57%	22.86%	51.43%	51.43%
complex vegetation water access	32	<b>0.00%</b>	0.00%	0.00%	0.00%	0.00%	0.00%
complex urban fire risk	32	12.50%	9.38%	<b>15.62%</b>	6.25%	15.62%	6.25%
complex urban flood risk	18	11.11%	11.11%	11.11%	0.00%	<b>16.67%</b>	5.56%
complex average	15	0.00%	<b>6.67%</b>	0.00%	6.67%	0.00%	0.00%
power calculation	14	<b>7.14%</b>	0.00%	7.14%	0.00%	0.00%	0.00%
binary threshold	11	<b>100.00%</b>	100.00%	100.00%	90.91%	100.00%	100.00%
binary presence	10	<b>100.00%</b>	100.00%	100.00%	100.00%	90.00%	50.00%
binary multiple	10	90.00%	<b>100.00%</b>	90.00%	100.00%	80.00%	60.00%
building fire risk	9	33.33%	33.33%	33.33%	22.22%	22.22%	<b>44.44%</b>
complex size filter	6	<b>66.67%</b>	0.00%	66.67%	0.00%	66.67%	0.00%
total area	6	0.00%	0.00%	0.00%	0.00%	<b>16.67%</b>	0.00%
building flood risk	4	50.00%	50.00%	50.00%	25.00%	<b>75.00%</b>	50.00%
Total	2000	42.00%	32.10%	36.90%	29.00%	28.10%	26.45%

Q-A: QVLM(GPT-5 + ConvNeXt); Q-B: QVLM(GPT-oss-120B + ConvNeXt); Q-C: QVLM(GPT-5 + DINOv3); Q-D: QVLM(llama3.1-8B + ConvNeXt); VLM-A: GPT-5; VLM-B: QWEN 30B A3B thinking

Table 11. **Full QVLM result (with Q-A setup) for one SQuID entry:** (A) one entry in SQuID, showing the question, corresponding image, expected answer and acceptable answer range; (B) corresponding image; (C) segmentation overlays; (D) LLM-generated code; (E) printout from code. The final answer (7) is within the acceptable range given in SQuID [4,8].

(B) SQuID image



(C) Segmentation overlays. Colors: agricultural (yellow), roofs (magenta).



(A) SQuID entry

```
{
  "id": "SQuID_11144",
  "image": "earthvqa_0.3m/2923.png",
  "question": "How many buildings (larger than 0.01 hectares) are within 200m of agricultural land? (GSD: 0.3m)",
  "answer": 6,
  "type": "building_proximity",
  "tier": 2,
  "gsd": 0.3,
  "acceptable_range": [ 4, 8 ]
},
```

(D) LLM-generated code

```
gsd = 0.3
# Segment image for agricultural land and roofs
# (buildings)
seg_result = segment_image_from_path(IMAGE_PATH,
                                      ["agric", "roof"], gsd=gsd)
shapes = seg_result["shapes"]
total_pixels = seg_result["total_pixels"]
# Separate shapes by class
agric_shapes = [s for s in shapes if s["class_type"] == "agric"]
roofs = [s for s in shapes if s["class_type"] == "roof"]
# Filter roofs by area > 0.01 hectares
min_hectares = 0.01
large_roofs = [s for s in roofs if
              s.get("area_hectares", 0) > min_hectares]
# Clip large roofs to portions within 200 m of any
# agricultural land
distance_m = 200.0
roofs_within =
    find_shapes_within_distance(large_roofs,
                                 agric_shapes, distance_m, resolution=gsd)
cnt_bldg_within = len(roofs_within)
# Print intermediate findings
print(f"Initial agric shapes: {len(agric_shapes)}")
print(f"Initial roof shapes: {len(roofs)}")
print(f"Large roofs (> {min_hectares} ha): {len(large_roofs)}")
print(f"Clipped roof within {distance_m} m of agric: {len(roofs_within)}")
print(f"Large buildings within {distance_m} m of agric: {cnt_bldg_within}")
answer = cnt_bldg_within
```

(E) printout from executing the code

```
Initial agric shapes: 1
Initial roof shapes: 13
Large roofs (> 0.01 ha): 7
Clipped roof parts within 200.0 m of agric: 7
Large buildings within 200.0 m of agric: 7
```